High-Temperature Phonon-Mediated Superconductivity with T_c above 100 K in Monolayer $Na(BC)_2$ and $K(BC)_2$

Wenxuan Chen(陈文轩), Zhengtao Liu(刘正涛), Zihao Huo(霍子豪), Guiyan Dong(董桂言), Jialiang Cai(蔡嘉良), and Defang Duan(段德芳)*

Key Laboratory of Material Simulation Methods & Software of Ministry of Education, and State Key Laboratory of Superhard Materials, College of Physics, Jilin University, Changchun 130012, China

(Received 19 August 2024; accepted manuscript online 10 October 2024)

Two-dimensional (2D) materials have demonstrated promising prospects owing to their distinctive electronic properties and exceptional mechanical properties. Among them, 2D superconductors with T_c above the boiling point of liquid nitrogen (77 K) will exhibit tremendous applicable value in the future. Here, we design two 2D superconductors $Na(BC)_2$ and $K(BC)_2$ with MgB_2-like structures, which are theoretically predicted to host T_c as high as 99 and 102 K, respectively. The origin of such high T_c is ascribed to the presence of both σ-bonding bands and van Hove singularity at the Fermi level. Furthermore, T_c of $Na(BC)_2$ is boosted up to 153 K with a biaxial strain of 5%, which sets a new record among 2D superconductors. The predictions of $Na(BC)_2$ and $K(BC)_2$ open the door to explore 2D high-temperature superconductors and provide a potential future for developing new applications in 2D materials.

DOI: 10.1088/0256-307X/41/11/117403

More and more two-dimensional (2D) materials, such as graphene,[1] silicene,[2,3] and transition metal dichalcogenide (TMD),[4–9] have attracted tremendous interests and have been widely studied due to their unique properties and potential applications. Due to the application prospects on nano devices, 2D superconducting materials play an irreplaceable role in nondissipative electronic devices, low dissipative integrated circuits, and imaging equipment.[10] One main challenge in 2D superconductors is that how to remain the superconductivity in most of the well-known conventional bulk superconductors when the dimensions are reduced.[11–16] Therefore, the exploration of 2D superconductors with higher T_c has become an important topic in condensed matter physics and material science.

Several families of 2D superconductor have been discovered in recent years. However, up to date, there are few 2D superconductors with T_c exceeding 77 K. Theoretical prediction suggested that the deposition of alkali metal atoms on graphene can effectively improve the electron–phonon coupling (EPC) and induce the superconductivity.[17–20] For example, LiC_6 and CaC_6 were predicted to host critical temperatures (T_c) of 8.1 and 1.4 K, respectively, and Li-decorated monolayer graphene was experimentally synthesized with a T_c of 5.9 K.[19] Meanwhile, other 2D material families, such as TMD[4–7] and MXene,[21–24] exhibit some interesting physical properties, but also host low T_c. For example, monolayer MoS_2 with a T_c of 3 K can be obtained by chemical exfoliation from millimeter-sized 1T' crystal[25] and is predicted to host a T_c of 22 K at the optimal hole doping concentration.[26] Such a low T_c greatly amplifies the expenses in the process of using devices, seriously limiting their applications.

Among all of the Bardeen–Cooper–Schrieffer (BCS) superconductors, bulk MgB_2,[27–29] with space group of $P6/mmm$, contains alternating layers of Mg and B atoms stacked along the $\boldsymbol{c}$ lattice direction and hosts the highest T_c (39 K) at ambient pressure in experiment.[27] Due to the layered structure, MgB_2 is a candidate to examine the behavior of superconductivity at the 3D-to-2D transition.[30] When its thickness gets down to monolayer, MgB_4 exhibits a very strong surface state, and its properties have a great change, which leads to four-gap superconductivity with T_c above 50 K.[31] Therefore, monolayer MgB_2 is considered to be a good template for designing 2D superconductors. It is suggested that monolayer MgB_2-like structures have the potential to achieve high-temperature superconductivity, such as NbB_2 and CaB_2 with T_c above 35 K.[32] Chemical doping can further improve the T_c based on monolayer MgB_2. For further improving its T_c and stability, substituting the intercalation is necessary and can effectively enhance the superconductivity. For example, a mono boron-carbon layer LiBC hosts a T_c of 65 K,[33] while a double boron-carbon layer LiB_2C_2 enhances the T_c to 90 K.[34] The hydrogenation of monolayer MgB_2 leads to a high T_c of 67 K, which can be further boosted to 103 K by biaxial tensile strain.[35]

In this work, we substitute the intercalation into alkali metal and design two 2D MgB_2-like superconductors $Na(BC)_2$ and $K(BC)_2$. The alkali metal intercalation effectively improves the stability of the B–C honeycomb and maximizes the content of boron and carbon. Such a strategy induces the presence of σ-bands crossing the Fermi

*Corresponding author. Email: duandf@jlu.edu.cn
© 2024 Chinese Physical Society and IOP Publishing Ltd

level and van Hove singularity (vHs), which stimulates strong EPC and significantly improves the T_c. We also explore the effect of biaxial strain to superconductivity and it is an effective method to adjust the T_c of 2D superconductors.

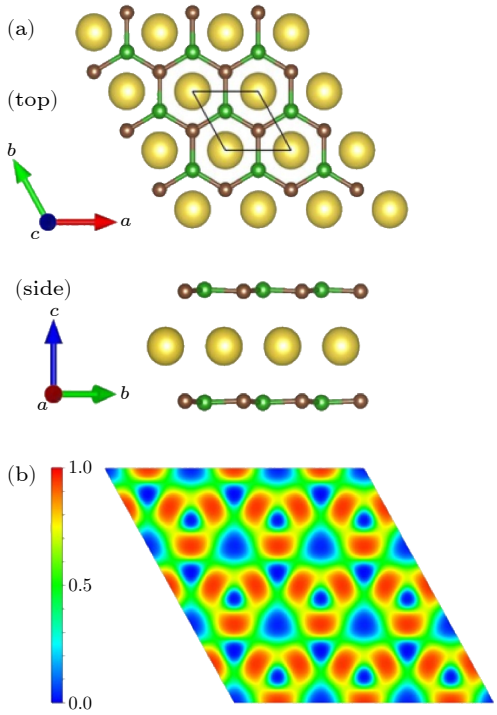

Fig. 1. (a) The crystal structure of 2D $Na(BC)_2$. (b) Two-dimensional ELF maps in ($h\,l\,k$ = 0, 0, 1) (top) planes of $Na(BC)_2$.

We designed two different structures of $X(BC)_2$ (X = Na and K) based on the arrangement of boron-carbon layers (see Fig. S1 in the Supplementary Material). Two boron-carbon layers are symmetrically arranged on either side of Na atoms. In the first structure, the B atom is positioned directly above the B atom on the other side, while the C atom is located above another C atom. In the other structure, the B atom is situated above the C atom and vice versa for the C atom, which is the same as the previously reported structure of LiB_2C_2. Our calculations reveal that the energy of the former is about 2 meV/f.u. lower than that of the latter for $Na(BC)_2$ and $K(BC)_2$ and the wrinkles in the former is likely to be the origin of the energy benefit. Therefore, we only consider and discuss the former structure. We also performed the crystal structure prediction implemented on the CALYPSO code [36,37] and confirmed this structure is energetically favorable. The stability of $Na(BC)_2$ and $K(BC)_2$ is studied from three aspects, including energy stability, thermal stability, and dynamical stability. We calculated the cohesive energy (E_{coh}) using the following formula:

$$E_{coh} = \frac{[E_{X(BC)_2} - (n_X E_X + n_B E_B + n_C E_C)]}{n_X + n_B + n_C},$$

where E_B, E_C, E_X and $E_{X(BC)_2}$ are the total energies of a single atom of B, C, X (X = Na, K) and one unit cell of $X(BC)_2$; n_X, n_C and n_B are the numbers of X, C and B atoms in a unit cell. The calculated E_{coh} values of $Na(BC)_2$ and $K(BC)_2$ are −6.318 eV/atom and −6.057 eV/atom, respectively, which are lower than the well-known silicene (−3.98 eV/atom) and germanene (−3.26 eV/atom),[38] indicating the feasibility of experimental synthesis. For the *ab initio* molecular dynamics (AIMD) simulations, the variation of free energy within 8 ps at 800 K and the last snapshot in top and side views are exhibited in Fig. S2 of the Supplementary Material. It maintains the structural integrity even at 800 K, proving their thermodynamical stability. Furthermore, the phonon spectra of $X(BC)_2$ are shown in Fig. 3. Obviously, there is no imaginary frequency in phonon spectrum, indicating their dynamical stability.

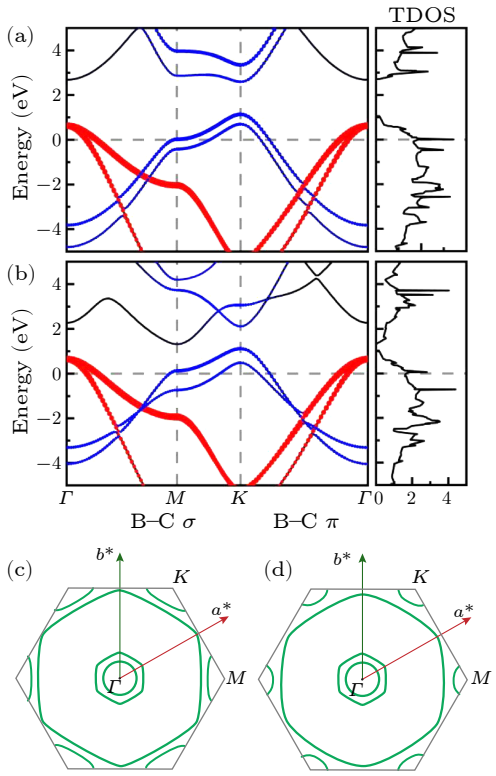

Fig. 2. Projected electronic band structures and total density of states (TDOS) of (a) $Na(BC)_2$ and (b) $K(BC)_2$. Fermi surfaces of (c) $Na(BC)_2$ and (d) $K(BC)_2$.

We used a variety of theoretical methods to study the relationship between electronic properties and superconductivity of $X(BC)_2$. We first examined the chemical bonding of 2D $Na(BC)_2$ by analyzing electron localization function (ELF). ELF values for the B–C bonds are above 0.7 [see Fig. 1(b)], showing the evidence for B–C covalent bonding, which is similar with other MgB_2-like materials. On the other hand, the strong orbital overlap of B and C atom also indicates a measure of the covalency in the B–C bond. To further comprehend the electronic properties of $X(BC)_2$, we also calculated their electronic band structures, density of states (DOS), and Fermi surfaces. As shown in Fig. 2, two σ bands crossing the Fermi level suggest the intrinsic metallic features of σ electrons in $X(BC)_2$. The σ band is usually filled with electrons and is below the Fermi level, which is non-conducting, such

as diamond[39] and hydrogen.[40] Due to the strong interaction between σ electrons and phonon, when the σ-bands are raised to the Fermi level through chemical doping or high pressure, these electrons will be coupled to the phonon to form superconducting electron pairs. For example, the σ band is metallized by high pressure in H_3S, which hosts a high T_c of 203 K at 155 GPa.[41,42] The metallic of σ electrons and σ band crossing the Fermi level is a characteristic of high-temperature superconductivity,[43] and it is suggested that $X(BC)_2$ are likely to be high-temperature superconductors. Interestingly, there is a flat π band along the high-symmetry M–K direction, inducing a vHs at the Fermi level, which is beneficial for superconductivity. We note that a similar vHs always appears at the M point in MgB_2-like materials,[32,33,44,45] but it is away from the Fermi level and has no effect to the superconductivity. The vHs at the Fermi level origins from π bonds and may be associated with out-plane vibrations, which is always not related to 2D superconductivity. However, it is likely to boost a high T_c for $X(BC)_2$. The Fermi contours of $X(BC)_2$ are shown in Figs. 2(c) and 2(d). A double ring hole pocket locates at the Γ point, which is derived from the σ orbitals, and a hexagonal pocket along the boundaries of Brillouin zones and a small ring pocket centered at the K point are derived from π orbitals.

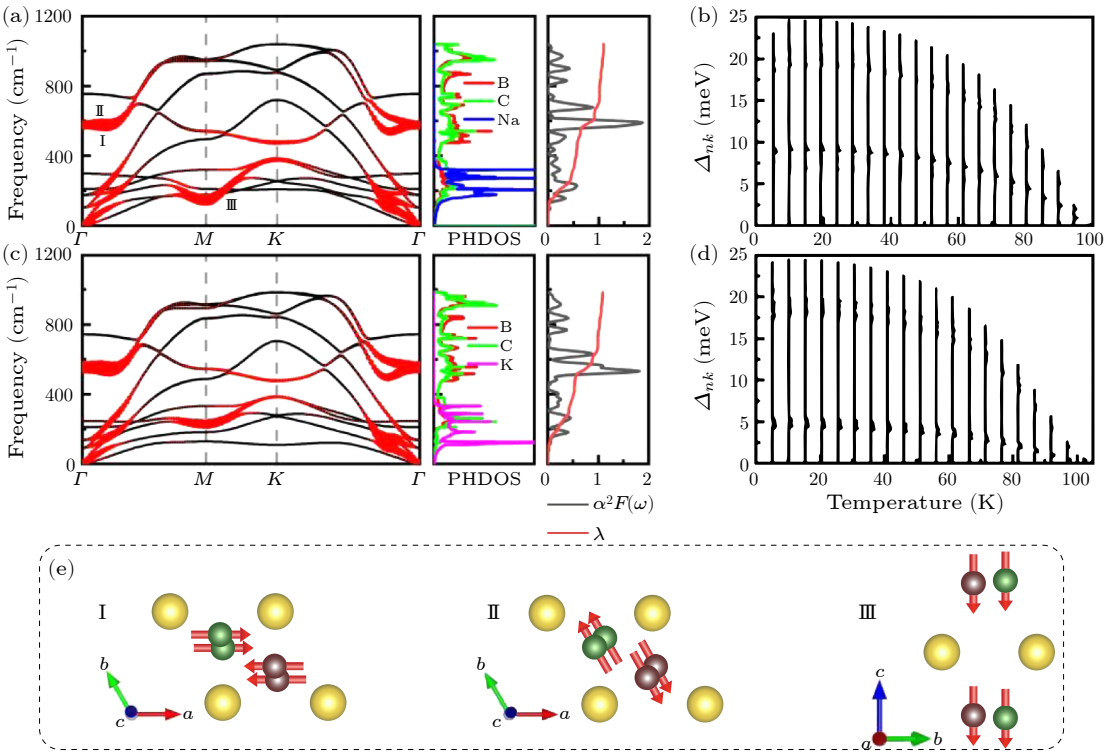

Fig. 3. Phonon dispersion curves (left), phonon density of states (middle), and Eliashberg spectral function $\alpha^2F(\omega)$ together with the electron–phonon integral λ (right) of (a) $Na(BC)_2$ and (c) $K(BC)_2$. Energy distribution of superconducting gaps Δ_{nk} versus T for (b) $Na(BC)_2$ and (d) $K(BC)_2$. (e) Phonon modes with the strongest EPC in $Na(BC)_2$, labeled as indicated in (a).

To explore the EPC and superconductivity of $X(BC)_2$, we calculated their phonon dispersion curves, phonon density of states, and Eliashberg spectral function $\alpha^2F(\omega)$, as shown in Fig. 3. For $Na(BC)_2$, it can be found that the low frequency region (below 400 cm^{-1}) in phonon spectrum is from the vibration of all elements, while the high frequency region (above 400 cm^{-1}) mainly comes from the vibration of boron and carbon. Note that the strong EPC strength is located at Γ point [see Fig. 3(a)], corresponding to some high peaks of Eliashberg functions $\alpha^2F(\omega)$ at around 600 cm^{-1}. It origins from the strong coupling between the σ electrons and the in-plane B–C stretching mode E_{2g} [see I and II in Fig. 3(e)], which is an important feature in MgB_2-like materials. However, different from MgB_2 and other MgB_2-like materials,[28,32,33] there is an obvious phonon softening at M point and the softening of acoustic branch effectively boosts the EPC strength. It is attributed to the π bonds and out-plane vibrations of B and C, as shown in III in Fig. 3(e), which is not common in 2D superconductors. The similar phenomenon appears in $K(BC)_2$. Compared to $Na(BC)_2$, we can find that the softening at M point is weaker in $K(BC)_2$, and the high frequency vibration induces a higher EPC at Γ point. It may origin from the larger atomic radius of K atom, and it will induce an in-plane stretching, which intensifies the in-plane vibrations. The vibrations of low and high frequencies contribute 49% and 51% to the total λ, respectively. The overall isotropic EPC constant values of $Na(BC)_2$ and $K(BC)_2$ are 1.10 and 1.09, respectively. For LiB_2C_2, we note that there is a flat band close to the Fermi level in the electronic band structure and a little phonon softening at M point.[34] Therefore, the adjustment of the vHs is

important on the enhance of EPC and superconductivity.

The anisotropy of superconductivity is important for 2D superconductors.[23,32,35,46] We further calculated the superconducting energy gaps (Δ_{nk}) of $Na(BC)_2$ and $K(BC)_2$ by solving anisotropic Migdal–Eliashberg equations.[47] The Coulomb repulsion parameter (μ^*) is taken as 0.10, which is a reasonable choice for the conventional superconductors.[28,44,48,49] Figures 3(b) and 3(d) show the temperature evolution of the superconducting gaps. A striking feature of $Na(BC)_2$ is the existence of two-gap superconductivity, and averaged values of superconducting gaps are about 9 and 20 meV at 5 K. We notice that the gaps are distinguishable at 99 K and 102 K for $Na(BC)_2$ and $K(BC)_2$, respectively, which are much higher than the boiling point of liquid nitrogen. It is suggested that a pristine monolayer of $K(BC)_2$ will be the first 2D-BCS superconductor with a record-breaking T_c above 100 K among pure 2D superconductors, without any tuning of external parameters such as charge doping, strain, or substrate induced effects. Through the above analysis, we believe that the σ bands crossing the Fermi level is the foundation of the high-temperature superconductivity in $X(BC)_2$, and the strong EPC attributed by the vHs at the Fermi level and out-plane vibration is likely to be the critical factor of their unprecedented T_c.

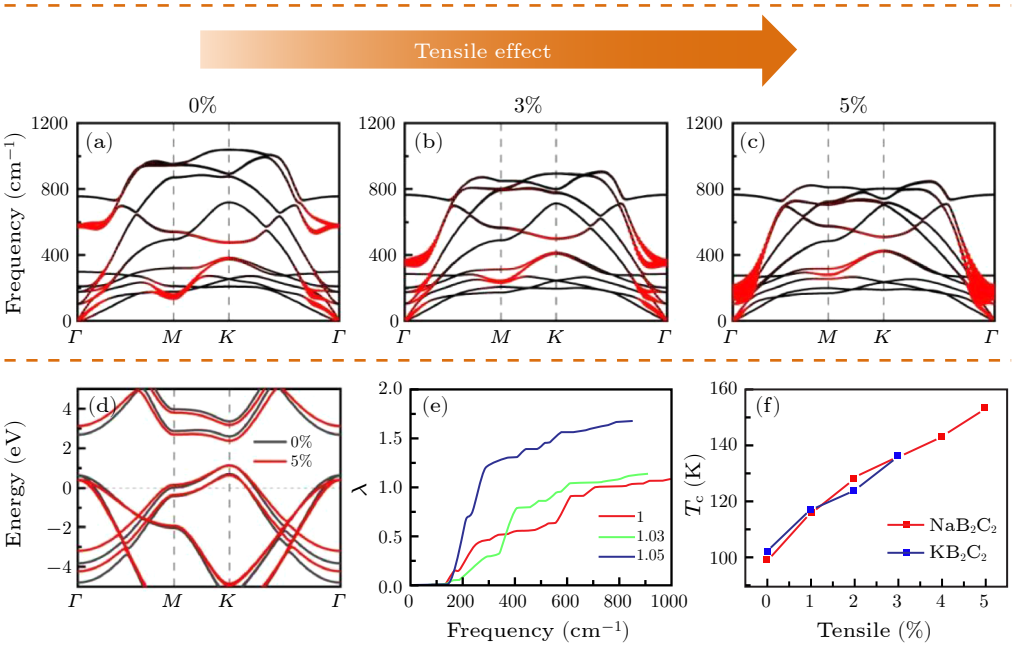

Fig. 4. Phonon dispersion curves of $Na(BC)_2$ with a biaxial strain of (a) 0%, (b) 3% and (c) 5%. (d) The electronic band structures of $Na(BC)_2$ with biaxial strains of 0% and 5%. Black lines and red lines represent the band structures with 0% and 5% strains, respectively. (e) EPC parameters λ for $Na(BC)_2$ under different biaxial strains. (f) T_c versus biaxial strain for $Na(BC)_2$ and $K(BC)_2$.

Strain engineering has been demonstrated as an effective way to regulate electronic and dynamical properties of 2D materials,[23,35,50] and it is found that the application of anisotropic mechanical stress is beneficial to the superconductivity in some diborides.[50] Thus, we applied in-plane biaxial strain to further improve the superconducting properties of $X(BC)_2$. By calculating the phonon spectrum with different strains, we found that $Na(BC)_2$ can be stable at up to 5% tensile strain. As shown in Fig. 4, it can be found that with the increase of tensile strain, the frequency of phonon vibration continues to decrease. There is obvious softening of E_{2g} mode near the Γ point and their frequencies decrease from 600 to 200 cm^{-1}. Such a phonon softening significantly improves the λ in the low-frequency region and it can be found that there is two rapidly improvements around 200 cm^{-1} in $Na(BC)_2$ with 5% tensile strain. Meanwhile, the softening of acoustic branch at M point weakens with the increasing biaxial strain and provides less EPC to the total λ. Electronic band structures show that 5% tensile strain can induce the σ-bands near the Γ point closer to the Fermi level and increase the DOS from σ-bands. The vHs gradually moves away from the Fermi level, which is associated with the weakening of EPC at the M point, and it is suggested that the σ-bands play a crucial role in the improvement of the T_c. By solving the anisotropic Migdal–Eliashberg equations,[47] we find that 5% tensile strain increases the Δ_{nk} of $Na(BC)_2$ at 5 K from 20 meV to 30 meV (see Fig. S3). With the increase of the strain, there is a linear relationship between the strain and T_c, reaching a maximum of 153 K at 5% tensile, which creates a new record for the T_c of 2D superconducting materials. A similar phenomenon occurs in $K(BC)_2$. The change of band structures and the softening of phonon in $K(BC)_2$ induce the enhancement of EPC. However, the larger atomic radius of K atom weakens the dynamical stability of $K(BC)_2$, resulting in a maximum strain of only 3%. As the strain increases, its T_c increases from 102 K to 136 K. The results show that biaxial strain

significantly improves the EPC and superconductivity.

Here, we compare superconducting parameters of $Na(BC)_2$ and $K(BC)_2$ with some well-known phonon-mediated 2D superconductors and list the data in Table 1. It is possible for graphene to achieve high-temperature superconductivity by p-type doping[51] or Be-decorated,[52] but the method is difficult in experiment and is almost impossible to achieve in applications. TMD superconductors have been extensively explored and have mature synthesis technology, while they always host low T_c. Hydrogenation of MoS_2 has been achieved experimentally[53,54] and is predicted to have a T_c of 29 K.[55] There are a few superconductors with such a high T_c even in monolayer MgB_2-like materials. For example, $Mg_2B_4C_2$,[44] LiBC,[33] and LiB_2C_2[34] host T_c of 41.6, 65, and 92 K, respectively. Recently, hydrogenated MgB_2 with 5% strain[35] and LiB_2C_2 with 8% strain[34] can reach high T_c above 100 K. Note that $Na(BC)_2$ host the highest T_c among these reported 2D superconductors, which exceeds that of hydrogenated MgB_2 and LiB_2C_2. Such a high T_c provides the possibility to explore superconducting devices in the liquid nitrogen temperature range. With the development of metal intercalation graphene technology,[17,18] monolayer materials with similar structures have great possibilities to be synthesized. The experimental synthesis and characterization of their excellent superconductivity in monolayer $Na(BC)_2$ and $K(BC)_2$ are highly expected in the future.

Table 1. Doping, biaxial strain ε, EPC constant λ, logarithmically averaged phonon frequency $\omega_{\log}$, and superconducting T_c for several 2D superconductors.

Materials	Doping	ε (%)	λ	$\omega_{\log}$ (cm^{-1})	T_c (K)	References
Graphene	4.65×10^{14} cm^{-2}	16.5	1.45	289.06	30.2	[56]
	10% p-type doping	0.0	1.45	909.35	91.1	[51]
LiC_6	0.0	0.0	0.61	400	8.1	[19]
CaC_6	0.0	0.0	0.40	445.64	1.4	[19]
AlC_8	0.20 hole/cell	12	1.557	188.45	22.23	[20]
B_2C	0.0	0.0	0.92	315	19	[57]
Mo_2C	0.0	0.0	0.63	–	5.9	[58]
MoSH	0.0	0.0	1.48	178.36	28.92	[55]
MgB_2	0.0	0.0	0.68	–	20	[59]
Hydrogenated	0.0	0.0	1.46	–	67	[35]
MgB_2	0.0	5.0	2.03	–	103.0	[35]
CaB_2	0.0	0.0	1.67	360.0	41.6	[32]
LiBC	0.0	0.0	0.59	–	65	[33]
$Mg_2B_4C_2$	0.0	0.0	1.40	506	47.2	[44]
BeC_2	0.0	0.0	4.07	224.3	72.1	[52]
LiB_2C_2	0.0	0.0	1.25	311.3	92	[34]
	0.0	8.0	1.52	384.1	125	[34]
$Na(BC)_2$	0.0	0.0	1.09	541.6	99	This work
	0.0	5.0	1.66	402.1	153	This work
$K(BC)_2$	0.0	0.0	1.08	552.7	102	This work
	0.0	3.0	1.47	464.0	136	This work

In summary, we theoretically predict two stable 2D superconductors $Na(BC)_2$ and $K(BC)_2$ with high T_c through intercalation substitution. The band structures suggest that the presence of σ-bands and vHs at the Fermi level are the signal of high temperature superconductivity. It is suggested that the phonon softening at Γ and M point are the common origin of their high-temperature superconductivity. The in-plane and out-plane vibrations boost a strong EPC together, and they host remarkably high T_c of 99 and 102 K, respectively. Biaxial strain significantly improves the T_c of $Na(BC)_2$ to 153 K and sets a new record in 2D superconductors. Such a high T_c is much higher than other 2D superconductors and represents a promising future of the application in 2D materials at or above liquid nitrogen temperature. Our predictions also provide a novel theoretical understanding for designing 2D superconductors with high T_c, and open the door to explore adjustment devices of 2D materials.

Note Added. We noted that during the preparation of our manuscript, the similar 2D structure was reported by two different groups.[60,61]

Acknowledgements. This work was supported by the National Natural Science Foundation of China (Grant Nos. 12122405 and 12274169), the National Key Research and Development Program of China (Grant Nos. 2022YFA1402304 and 2023YFA1406200), and the Fundamental Research Funds for the Central Universities. Some of the calculations were performed at the High-Performance Computing Center of Jilin University and using TianHe-1(A) at the National Supercomputer Center in Tianjin.

References

[1] Novoselov K S, Geim A K, Morozov S V, Jiang D, Zhang Y, Dubonos S V, Grigorieva I V, and Firsov A A 2004 *Science* **306** 666
[2] Cahangirov S, Topsakal M, Aktürk E, Şahin H, and Ciraci S 2009 *Phys. Rev. Lett.* **102** 236804
[3] Chen L, Liu C C, Feng B, He X, Cheng P, Ding Z, Meng S, Yao Y, and Wu K 2012 *Phys. Rev. Lett.* **109** 056804

[4] Chhowalla M, Shin H S, Eda G, Li L J, Loh K P, and Zhang H 2013 *Nat. Chem.* **5** 263
[5] Mak K F, Lee C, Hone J, Shan J, and Heinz T F 2010 *Phys. Rev. Lett.* **105** 136805
[6] Feng J, Peng L, Wu C, Sun X, Hu S, Lin C, Dai J, Yang J, and Xie Y 2012 *Adv. Mater.* **24** 1969
[7] Yan L M, Ding C, Li M T, Tang R L, Chen W, Liu B Y, Bu K J, Huang T H, Dai D Z, Jin X B, Yang X F, Cheng E J, Li N N, Zhang Q, Liu F L, Liu X Q, Zhang D Z, Ma S L, Tao Q, Zhu P W, Li S Y, Lü X J, Sun J, Wang X, and Yang W G 2023 *Nano Lett.* **23** 2121
[8] Dong L, Wang G Y, Zhu Z, Zhao C X, Yang X Y, Li A M, Chen J L, Guan D D, Li Y Y, Zheng H, Xie M H, and Jia J F 2018 *Chin. Phys. Lett.* **35** 066801
[9] Xie X, Lin D, Zhu L, Li Q, Zong J, Chen W, Meng Q, Tian Q, Li S C, Xi X, Wang C, and Zhang Y 2021 *Chin. Phys. Lett.* **38** 107101
[10] Ichinokura S, Nakata Y, Sugawara K, Endo Y, Takayama A, Takahashi T, and Hasegawa S 2019 *Phys. Rev. B* **99** 220501
[11] Frindt R F 1972 *Phys. Rev. Lett.* **28** 299
[12] Xi X X, Zhao L, Wang Z F, Berger H, Forró L, Shan J, and Mak K F 2015 *Nat. Nanotechnol.* **10** 765
[13] Ugeda M M, Bradley A J, Zhang Y, Onishi S, Chen Y, Ruan W, Ojeda-Aristizabal C, Ryu H, Edmonds M T, Tsai H Z, Riss A, Mo S K, Lee D, Zettl A, Hussain Z, Shen Z X, and Crommie M F 2016 *Nat. Phys.* **12** 92
[14] Xi X, Wang Z, Zhao W, Park J H, Law K T, Berger H, Forró L, Shan J, and Mak K F 2015 *Nat. Phys.* **12** 139
[15] Bao L, Bi Y, Liu X, Yang X, Hao T, Tian S, Wang Z, Li J, and Gu C 2018 *Appl. Phys. Lett.* **113** 022603
[16] Yang Q, Jiang X, and Zhao J 2023 *Chin. Phys. Lett.* **40** 107401
[17] Ichinokura S, Sugawara K, Takayama A, Takahashi T, and Hasegawa S 2016 *ACS Nano* **10** 2761
[18] Xue M, Chen G, Yang H, Zhu Y, Wang D, He J, and Cao T 2012 *J. Am. Chem. Soc.* **134** 6536
[19] Profeta G, Calandra M, and Mauri F 2012 *Nat. Phys.* **8** 131
[20] Lu H Y, Yang Y, Hao L, Wang W S, Geng L, Zheng M, Li Y, Jiao N, Zhang P, and Ting C S 2020 *Phys. Rev. B* **101** 214514
[21] Bekaert J, Sevik C, and Milošević M V 2022 *Nanoscale* **14** 9918
[22] Tsuppayakorn-Aek P, Bovornratanaraks T, Ahuja R, Luo W, and Kotmool K 2023 *Phys. Chem. Chem. Phys.* **25** 2227
[23] Campi D, Kumari S, and Marzari N 2021 *Nano Lett.* **21** 3435
[24] Yin X Z, Wang H, Wang Q H, Jiao N, Ni M Y, Zheng M M, Lu H Y, and Zhang P 2023 *Chin. Phys. Lett.* **40** 097404
[25] Peng J, Liu Y, Luo X, Wu J, Lin Y, Guo Y, Zhao J, Wu X, Wu C, and Xie Y 2019 *Adv. Mater.* **31** 1900568
[26] Zeng S, Zhao Y, Li G, and Ni J 2016 *Phys. Rev. B* **94** 024501
[27] Nagamatsu J, Nakagawa N, Muranaka T, Zenitani Y, and Akimitsu J 2001 *Nature* **410** 63
[28] Choi H J, David R, Sun H, Marvin L C, and Louie S G 2002 *Nature* **418** 758
[29] Kang W N, Kim H J, Choi E M, Jung C U, and Lee S I 2001 *Science* **292** 1521
[30] Xu B Z and Beckman S P 2016 *2D Mater.* **3** 031003
[31] Zhao Y, Lian C, Zeng S, Dai Z, Meng S, and Ni J 2020 *Phys. Rev. B* **101** 104507
[32] Sevik C, Bekaert J, Petrov M, and Milošević M V 2022 *Phys. Rev. Mater.* **6** 024803
[33] Modak P, Verma A K, and Mishra A K 2021 *Phys. Rev. B* **104** 054504
[34] Gao M, Yan X W, Lu Z Y, and Xiang T 2020 *Phys. Rev. B* **101** 094501
[35] Bekaert J, Petrov M, Aperis A, Oppeneer P M, and Milošević M V 2019 *Phys. Rev. Lett.* **123** 077001
[36] Wang Y, Lv J, Zhu L, and Ma Y 2012 *Comput. Phys. Commun.* **183** 2063
[37] Wang Y, Lv J, Zhu L, and Ma Y 2010 *Phys. Rev. B* **82** 094116
[38] Yang L M, Bačić V, Popov I A, Boldyrev A I, Heine T, Frauenheim T, and Ganz E 2015 *J. Am. Chem. Soc.* **137** 2757
[39] Liu C, Song X, Li Q, Ma Y, and Chen C 2019 *Phys. Rev. Lett.* **123** 195504
[40] Song X, Liu C, Li Q, Hemley R J, Ma Y, and Chen C 2022 *Proc. Natl. Acad. Sci. USA* **119** e2122691119
[41] Drozdov A P, Eremets M I, Troyan I A, Ksenofontov V, and Shylin S I 2015 *Nature* **525** 73
[42] Einaga M, Sakata M, Ishikawa T, Shimizu K, Eremets M I, Drozdov A P, Troyan I A, Hirao N, and Ohishi Y 2016 *Nat. Phys.* **12** 835
[43] Gao M, Lu Z Y, and Xiang T 2015 *Phys. Rev. B* **91** 045132
[44] Singh S, Romero A H, Mella J D, Eremeev V, Muñoz E, Alexandrova A N, Rabe K M, Vanderbilt D, and Muñoz F 2022 *npj Quantum Mater.* **7** 37
[45] Yang L, Li Y P, Liu H D, Jiao N, Ni M Y, Lu H Y, Zhang P, and Ting C S 2023 *Chin. Phys. Lett.* **40** 017402
[46] Mannix A J, Zhou X F, Kiraly B, Wood J D, Alducin D, Myers B D, Liu X L, Fisher B L, Santiago U, Guest J R, Yacaman M J, Ponce A, Oganov A R, Hersam M C, and Guisinger N P 2015 *Science* **350** 1513
[47] Margine E R and Giustino F 2013 *Phys. Rev. B* **87** 024505
[48] Duan D, Liu Y, Tian F, Li D, Huang X, Zhao Z, Yu H, Liu B, Tian W, and Cui T 2014 *Sci. Rep.* **4** 6968
[49] Peng F, Sun Y, Pickard C J, Needs R J, Wu Q, and Ma Y 2017 *Phys. Rev. Lett.* **119** 107001
[50] Zhai H, Munoz F, and Alexandrova A N 2019 *J. Mater. Chem. C* **7** 10700
[51] Savini G, Ferrari A C, and Giustino F 2010 *Phys. Rev. Lett.* **105** 037002
[52] Yang L, Liu P F, Liu H D, Li Y P, Jiao N, Lu H Y, Wang B T, and Zhang P 2024 *Sci. China Phys. Mech. Astron.* **67** 217412
[53] Lu A Y, Zhu H, Xiao J, Chuu C P, Han Y, Chiu M H, Cheng C C, Yang C W, Wei K H, Yang Y, Wang Y, Sokaras D, Nordlund D, Yang P, Muller D A, Chou M Y, Zhang X, and Li L J 2017 *Nat. Nanotechnol.* **12** 744
[54] Wan X, Chen E, Yao J, Gao M, Miao X, Wang S, Gu Y, Xiao S, Zhan R, Chen K, Chen Z, Zeng X, Gu X, and Xu J 2021 *ACS Nano* **15** 20319
[55] Liu P F, Zheng F, Li J, Si J G, Wei L, Zhang J, and Wang B T 2022 *Phys. Rev. B* **105** 245420
[56] Si C, Liu Z, Duan W, and Liu F 2013 *Phys. Rev. Lett.* **111** 196802
[57] Dai J, Li Z, Yang J, and Hou J 2012 *Nanoscale* **4** 3032
[58] Zhang J J, and Dong S 2017 *J. Chem. Phys.* **146** 034705
[59] Bekaert J, Aperis A, Partoens B, Oppeneer P M, and Milošević M V 2017 *Phys. Rev. B* **96** 094510
[60] Meng X H, Shen Y Q, Lv L L, Zhou M, Yang X, Zhang Y, Pang L, E P, and Zhou Z X 2024 *Mater. Today Phys.* **47** 101532
[61] Zhang Y, Chen J, Hao J, Xu M, and Li Y 2024 *Phys. Rev. B* **110** 064513